Food Chemistry: X 27 (2025) 102408

Contents lists available at ScienceDirect

Food Chemistry: X

journal homepage: www.sciencedirect.com/journal/food-chemistry-x

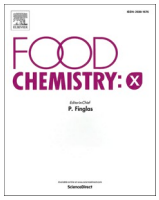

Characterizing flavor determinants and α-glucosidase inhibitory components in ancient tea plants and '*Qiancha 1*' white teas

Shimao Fang [a,b], Wenjing Huang [c], Xujun Zhu [b], Yuanchun Ma [b], Jingzhou Ran [d], Qiang Shen [a,*], Wanping Fang [b,**]

[a] *Guizhou Tea Research Institute, Guizhou Academy of Agricultural Sciences, Guiyang 550006, Guizhou, China*
[b] *College of Horticulture, Nanjing Agricultural University, Nanjing 210095, China*
[c] *National Key Laboratory for Tea Plant Germplasm Innovation and Resource Utilization, Anhui Agricultural University, Hefei 230036, China*
[d] *Guizhou Yanhe Wujiang ancient tea Co., LTD, Tongren 565322, China*

ARTICLE INFO

Keywords:
Ancient tea plants
Qiancha 1
White tea
α-Glucosidase
Flavor quality

ABSTRACT

This study aimed to compare white teas derived from ancient tea plants (AT) and the cultivar '*Qiancha 1*' (QC1) using multi-omics approaches, focusing on differences in volatile/non-volatile components, sensory traits, and α-glucosidase inhibitory activity. Both teas shared sweet aromas and mellow tastes, but AT exhibited significantly stronger floral intensity ($p < 0.05$), whereas QC1 dominated in citrus/fruity aroma. GC-olfactometry and chemometric modeling identified six key metabolites, with trans-β-ionone (rOAV = 149.6) and β-damascenone (rOAV = 47.6) driving floral and citrus/fruity characteristics, respectively. Targeted metabolomics revealed significantly higher levels of ester-catechins, caffeine, and gallic acid in AT. These compounds exhibited significant dose-response correlations with bitterness, astringency, and α-glucosidase inhibitory activity (r = 0.83–0.93, $p < 0.05$), suggesting their dual role in flavor enhancement and hypoglycemic potential. This work provides scientific evidence and technical insights for the high-value utilization of ancient tea plants resources and the optimization of white tea processing technologies.

1. Introduction

Tea is, after water, the world's most popular beverage, and offers a wealth of health benefits. Aroma and taste, which are the core sensory evaluation metrics, directly influence consumer acceptance and the potential for market premium (Yang et al., 2021). Modern research indicates that tea's characteristic flavors form through specific concentration thresholds and synergistic interactions of aroma and taste compounds (Guichard et al., 2019). These compounds' composition variations are collectively regulated by genetic background, cultivation environment, and processing techniques (Zhou et al., 2023). Thus, understanding tea flavor quality's molecular basis is vital for optimizing production processes, enhancing sensory quality, and aligning with consumers' evolving preferences.

White tea, a lightly fermented tea with a sweet-mellow flavor, has its flavor quality influenced by cultivar, processing, and storage (Zhou et al., 2023). Comparative analyses show *CaiCha*-processed white teas have significantly higher aromatic compounds and saccharide concentrations than *Fuding Dabai*-produced ones, yielding stronger floral-fruity aromas and sweeter profiles (Lin, Huang, et al., 2024). Processing optimization reveals solar withering and controlled stacking thickness activate terpenoid biosynthesis pathways, upregulating key enzymes like geranyl pyrophosphate synthase and alcohol dehydrogenase to boost floral-fruity volatiles (Lin, Dai, et al., 2024; Wu et al., 2024). Withering's water loss stress inhibits flavonoid glycosides (FGs) synthesis and induces degradation, improving taste acceptability. Drying further reduces FGs content, with lower temperatures (60 °C) optimally decreasing FGs, lessening bitterness, and preserving sweetness and umami for high sensory acceptance (Wang, Gao, et al., 2024; Wang, Liang, et al., 2024). Post-production microbial activity drives flavonoid/amino acid conversion, enhancing taste complexity (Zhang et al., 2024), while aroma quality sees reduced floral traits and increased herbal and aged odors (Huang et al., 2024). Moreover, white tea shows potential preventive and therapeutic effects against various diseases (Abiri et al., 2023; Tek et al., 2024). For example, tea's recently identified bioactive compounds, N-ethyl-2-pyrrolidinone-substituted flavan-3-ols (EPSFs),

* Corresponding author at: Tea Research Institute, Guizhou Academy of Agricultural Sciences, Guiyang 550006, Guizhou, China.
** Corresponding author at: College of Horticulture, Nanjing Agricultural University, Nanjing 210095, China.
E-mail addresses: shenqiang_gzu@163.com (Q. Shen), fangwp@njau.edu.cn (W. Fang).

https://doi.org/10.1016/j.fochx.2025.102408
Received 4 March 2025; Received in revised form 19 March 2025; Accepted 20 March 2025
Available online 25 March 2025

accumulate during white tea storage (Chen et al., 2024). Animal studies reveal EPSFs-rich white tea effectively alleviates colitis and hepatic fibrosis, likely by maintaining the hepatic oxidative-antioxidant system balance (Lin et al., 2024; Yılmaz et al., 2024).

Ancient tea plants (*Camellia sinensis* var. *sinensis*, defined as tea plants with an age ≥ 100 years) serve as a living gene bank for investigating the domestication origins of tea plants (Fang et al., 2024; Kong et al., 2025). Through long-term natural selection, they have developed unique metabolic regulation networks that differ from those of cultivated varieties (Peng et al., 2021; Yu et al., 2020). In previous work, we revealed the dynamic evolution of sensory characteristics and chemical composition during black tea processing from ancient tea plants. Our analysis demonstrated that the contents of ester-catechins (e.g., EGCG and ECG) and soluble sugars (e.g., sucrose and fructose) in fresh leaves exhibit significant positive correlations with the bitterness and sweetness of the final product, respectively (Fang et al., 2024). However, no systematic studies exist on the quality formation mechanism of white tea from ancient tea plants (AT). Current AT flavor evaluation systems rely on descriptive sensory terminology, lacking models that link key taste/aroma compounds to sensory attributes. This knowledge gap has dual consequences: First, the targeted regulation of metabolites during processing lacks theoretical guidance, resulting in compromised product quality consistency; second, process optimization is constrained by empirical approaches, hindering the efficient utilization of ancient tea plants resources. Therefore, elucidating the relationship between characteristic metabolites and flavor quality in ancient tea plants is critical for developing standardized processing technologies and enhancing product value.

This study used ancient tea plants (*Camellia sinensis* cv. *Qiancha 1*) from Yanhe County, Guizhou Province, and the cultivated elite cultivar '*Qiancha 1*' as raw materials (Qiao et al., 2025). White tea samples were produced under standardized processing conditions, which included program-controlled withering and temperature-gradient drying. An integrated approach involving multiple omics technologies was used: (1) headspace solid-phase microextraction coupled with gas chromatography/mass spectrometry (HS-SPME-GC/MS) for the quantitative analysis of volatile organic compounds (VOCs); (2) gas chromatography-olfactometry-mass spectrometry (GC-O-MS) to identify aroma-active compounds; (3) high-performance liquid chromatography (HPLC) to characterize non-volatile taste compounds; and (4) quantitative descriptive analysis (QDA) to establish models correlating sensory and chemical properties. By systematically analyzing the characteristic aroma molecular markers and key taste components of AT, this study clarifies the mechanisms underlying AT's quality differences from cultivated elite varieties. Furthermore, we established a novel flavor-chemical fingerprint for AT, providing a scientific foundation for resource authentication, process refinement, and functional product development.

2. Materials and methods

2.1. Sample collection

In July 2024, fresh leaves (*Camellia sinensis* var. *sinensis* (L.) O. Kuntze), with a picking standard of one bud and two leaves were collected from Tangba Town, Yanhe County, Guizhou Province (29°00′18″ N 108°14′01″ E; altitude 700–800 m) (Fig. S1). Fresh leaves (500 g per tray) were evenly spread across 10-layer trays in a program-controlled integrated device used for processing. Leaves from ancient tea plants and the cultivar '*Qiancha 1*' were alternately arranged on trays (excluding top and bottom layers). The spreading process was carried out under static conditions with a 10 mm ventilation gap on the equipment door. A staged temperature-humidity control program was implemented as follows: Phase 1: 28 °C ambient temperature with forced-air ventilation (10 min). Phase 2: Ventilation stopped, and leaves were incubated statically at 20 °C (2 h). This ventilation-incubation cycle was repeated until leaf edges transitioned from dark green to brown-black. The total withering duration was approximately 30 h. Hot air dehydration was performed under two conditions: 100 °C (20 min) and 80 °C (30 min). Throughout the dehydration process, a 10 mm gap was maintained on the chamber door of the equipment to facilitate the dissipation of water vapor and volatile compounds with odors (e.g., grassy odors) generated during treatment. The samples were dried at a constant temperature of 60 °C (3 h), subsequently cooled to room temperature, and sealed in duplicate aluminum foil bags. One portion was reserved for sensory evaluation, while the other was ground using a grinder, passed through a 40-mesh standard sieve, and stored at −20 °C for subsequent analysis.

2.2. Hs-SPME

Tea powder (3.0 g) was accurately weighed into a 250 mL stopper-equipped conical flask. Boiling ultrapure water (150 mL) was immediately poured into the flask, which was then stoppered and steeped for 5 min. The tea infusion was filtered through 400-mesh gauze and quickly cooled to room temperature in an ice-water bath. A 10 mL aliquot of the infusion was transferred to a 20 mL screw-threaded headspace vial. Subsequently, 10 μL of internal standard solution (decanoic acid ethyl ester, 10 μg/mL), 3.0 g sodium chloride, and a magnetic stir bar were sequentially added. The vial was immediately crimp-sealed with a septum made of PTFE and white silicone and vortex-mixed to ensure complete dissolution of sodium chloride. The headspace system was equilibrated under stirring in a 30 °C water bath for 15 min, after which the SPME fiber was inserted into the vial's headspace for 30 min adsorption of volatile compounds. Upon completion of adsorption, the fiber was immediately injected into the GC inlet for 5 min thermal desorption. All experimental procedures were performed in triplicate.

2.3. GC–MS instrument set-up and analytical conditions

The volatile compounds extracted by SPME were separated and identified using an Agilent 7890B gas chromatograph coupled with a 5977B mass spectrometer. Separation was performed on a DB-5MS capillary column (30 m × 0.25 mm × 0.25 μm) with helium (>99.999 % purity) as the carrier gas. All SPME analyses were conducted in splitless mode. The temperature program for the GC oven was set as follows: an initial hold at 40 °C for 5 min, followed by a ramp to 230 °C at 5 °C/min with a 5 min hold, and then an increase to 250 °C at 15 °C/min. The mass spectrometer operated in positive ion mode with a mass scan range of 30–350 *m/z* and an electron impact energy of 70 eV. Linear retention indices, which are used to help identify compounds in chromatography, were calculated using a C6-C40 n-alkane standard mixture. Compound identification was achieved by spectral matching with the NIST database and deconvolution analysis using AMDIS software. Relative quantification of volatile compounds was performed using decanoic acid ethyl ester as the internal standard. Detailed information on all reference odorants is available in our published work (Huang et al., 2022).

2.4. Identification of odorants through GC-O-MS

The GC-O-MS system (Agilent 8890 GC) was equipped with a mass spectrometer and olfactory port. The effluent from the analytical column was split into two equal flows in a 1:1 ratio: 50 % to the MS detector (250 °C) and 50 % to the olfactory port (230 °C). High-purity helium (>99.999 %) was used as the carrier gas with a linear velocity of 40 cm/s. The parameters for volatile compound separation and detection were consistent with those described in Section 2.3. To systematically characterize the aroma profiles and their intensity dynamics throughout the chromatographic separation, twelve trained panelists, with specialized sensory evaluation expertise, continuously monitored and recorded the aroma characteristics using a time-intensity protocol. A compound was

considered positively identified when its aroma signature was independently detected by at least two of the three panelists within the corresponding chromatographic retention window (Huang et al., 2022).

2.5. α-Glucosidase inhibition assay

The enzymatic activity was determined by hydrolysis of 4-nitrophenyl-β-D-glucopyranoside (PNPG) to p-nitrophenol (pNP). Under alkaline conditions, pNP exhibits maximum absorbance at 405 nm, which enabling quantification of inhibition efficiency by measuring pNP concentration using a microplate reader. The assay was adapted from Huang et al. (2025) with modifications. α-Glucosidase (0.5 U/mL) was prepared using 0.5 mol/L PBS buffer (pH 6.8). In a 96-well plate, 100 μL PBS buffer (0.5 mol/L, pH 6.8) and 20 μL α-glucosidase (0.5 U/mL) were mixed with 20 μL inhibitor (tea extract or acarbose) and incubated at 37 °C for 15 min. Subsequently, 20 μL PNPG (2.5 mmol/L) was added to initiate the reaction at 37 °C for 20 min, and then terminated by adding 80 μL Na_2CO_3 (5 mmol/L). Absorbance at 405 nm (controlOD) was measured using a microplate reader. Controls included: Blank: Reaction mixture without enzyme(controlOD). Negative control: Reaction mixture without inhibitor. Positive control: Acarbose solution. The enzyme inhibition rate (%) was calculated as:

$$\text{Inhibition rate}\ (\%) = 1 - \frac{(\text{ODtest} - \text{ODblank})}{\text{controlODtest} - \text{controlODblank}} \times 100$$

2.6. Sensory evaluation and QDA

The sensory evaluation and QDA were conducted in accordance with the procedures detailed in our previously published paper (Huang et al., 2022). The samples were prepared as described, and the traditional sensory evaluation was conducted in accordance with Chinese National Standard GB/T 23776–2018. The analysis was performed by a panel of twelve certified panelists, comprising six females and six males, all of whom held senior tea sensory evaluation certificates. QDA, a method to characterize the sensory properties of products, was conducted by twelve trained evaluators (six males and six females) to characterize the aroma and taste profiles of the tea infusions. Through consensus sessions, five aroma descriptors that are most representative of white tea were identified: flowery/honey-like, citrus/fruity, green/grassy, sweet, and fatty. At the same time, five representative descriptions of white tea taste were identified: sweet, umami, mellow, astringent and bitter. Each aroma and taste intensity were rated on a 4-point intensity scale (scores recorded to one-decimal-place precision): weak (0–1), moderate (>1–2), and intense (>2–4). All sensory data were collected for statistical analysis.

2.7. Determination of catechins, caffeine and gallic acid by HPLC

Tea powder (0.200 g) was mixed with 5 mL of preheated 70 % methanol (*v*/v) at 70 °C in a 10 mL centrifuge tube. The mixture was then homogenized and subjected to 70 °C water bath extraction for 10 min, and manual agitation every 5 min, followed by centrifugation at 3500 ×*g* for 10 min. The pellet was re-extracted using the same procedure, and the combined supernatants were brought to a final volume of 10 mL. The extract was diluted 5-fold with a stabilizing solution (containing 250 mg EDTA-2Na, 250 mg ascorbic acid, 50 mL acetonitrile, and adjusted to 500 mL with ultrapure water), filtered through a 0.22-μm membrane filter, and transferred to vials for HPLC analysis. Chromatographic conditions were consistent with our previously reported method (Fang et al., 2019).

2.8. Statistical analysis

Statistical analyses, including independent samples *t*-tests and PCA, were performed using SPSS. Redundancy analysis (RDA) was employed to explore variable relationships, and differential metabolite analysis was conducted using R. All results were visualized with Origin 2025 and R, which are widely applied in data analysis and visualization. The experimental design included three biological replicates, and quantitative data expressed as mean ± standard deviation. Statistical significance thresholds were consistent with biological research conventions: $^{*}p < 0.05$ (significant), $^{**}p < 0.01$ (very significant), and $^{***}p < 0.001$ (extremely significant).

3. Results and discussion

3.1. Flavor profile of AT and QC1 determined through QDA of sensory evaluation

This study utilized one-bud-two-leaf raw materials belonging to Bai Mudan-style white tea. According to the sensory evaluation results presented in Table S1, white teas processed from AT and QC1 fresh leaves under identical conditions exhibited similar flavor profiles, with quality characteristics consistent with the specifications stipulated in the GB/T 22291. Sensory analysis revealed that the dried tea leaves of AT displayed a grayish-green colour with a darker hue compared with the lighter grayish-green of QC1. The liquor colors were respectively apricot-yellow (AT) and light apricot-yellow (QC1) (Fig. 1A). QDA a comprehensive sensory evaluation technique integrating analytical and descriptive functions, has demonstrated significant advantages in quantifying tea sensory quality (Zhai et al., 2022). Aroma quantification (Fig. 1C) showed no statistical differences in sweet (2.45 vs. 2.51) or fatty odor (1.12 vs. 1.08) between the two samples ($p > 0.05$), both characterized by typical sweet odor profiles. However, AT exhibited significantly higher floral/honey-like (2.23 vs. 1.52, $p < 0.001$), whereas QC1 showed dominant citrus/fruity (2.92 vs. 1.90) and green/grassy odor (2.05 vs. 1.51) ($p < 0.001$). In terms of taste quality (Fig. 1D), no significant differences were found in sweetness (2.85 vs. 2.79) or mellow texture (2.12 vs. 2.09) ($p > 0.05$), both sharing a refreshing sweetness aftertaste. Notably, AT exhibited stronger bitterness (2.09 vs. 1.60) and astringency (1.89 vs. 1.38) ($p < 0.01$), while QC1 demonstrated superior umami (2.39 vs. 1.77, $p < 0.001$). The formation of tea flavor profiles is closely related to metabolite concentrations, sensory thresholds, and their synergistic interactions (Guichard et al., 2019; Zhai et al., 2022). QDA analysis confirmed significant sensory divergences between the two white teas processed from distinct raw materials under standardized conditions, which suggests potential differences in metabolite accumulation patterns between ancient tea plants and '*Qiancha 1*' fresh leaves.

3.2. Characterization of aroma compounds in AT and QC1 infusions via HS-SPME-GC/MS

The VOCs in the infusions of AT and QC1 white teas were analyzed using HS-SPME-GC/MS (Fig. 1B). Compound identification was rigorously verified through a triple verification system, including NIST mass spectral library matching (similarity >85 %), consistency analysis of characteristic ion fragments, and retention index calculations. As detailed in Table S2, a total of 80 VOCs were detected, with 79 compounds identified in AT and 80 in QC1. Notably, (E)-2-pentenal, a characteristic fruity, strawberry odor (María et al., 2002), was solely detected in QC1 at a concentration of 0.17 ± 0.03 μg/L. The detected compounds were classified into eight categories (Fig. 2), ranked according to number of compounds in descending order: terpenes (24 species, 30.00 %), aldehydes (20 species, 25.00 %), alcohols (11 species, 13.75 %), ketones (10 species, 12.50 %), heterocyclic compounds (7 species, 8.75 %), aromatic (5 species, 6.25 %), esters (2 species, 2.50 %), and sulfur-containing compounds (1 species, 1.25 %).

Quantification of total VOCs revealed that AT exhibited significantly higher total content (109.50 ± 3.11 μg/L) compared to QC1 (99.41 ± 5.38 μg/L) ($p < 0.05$, independent samples *t*-test). Differential

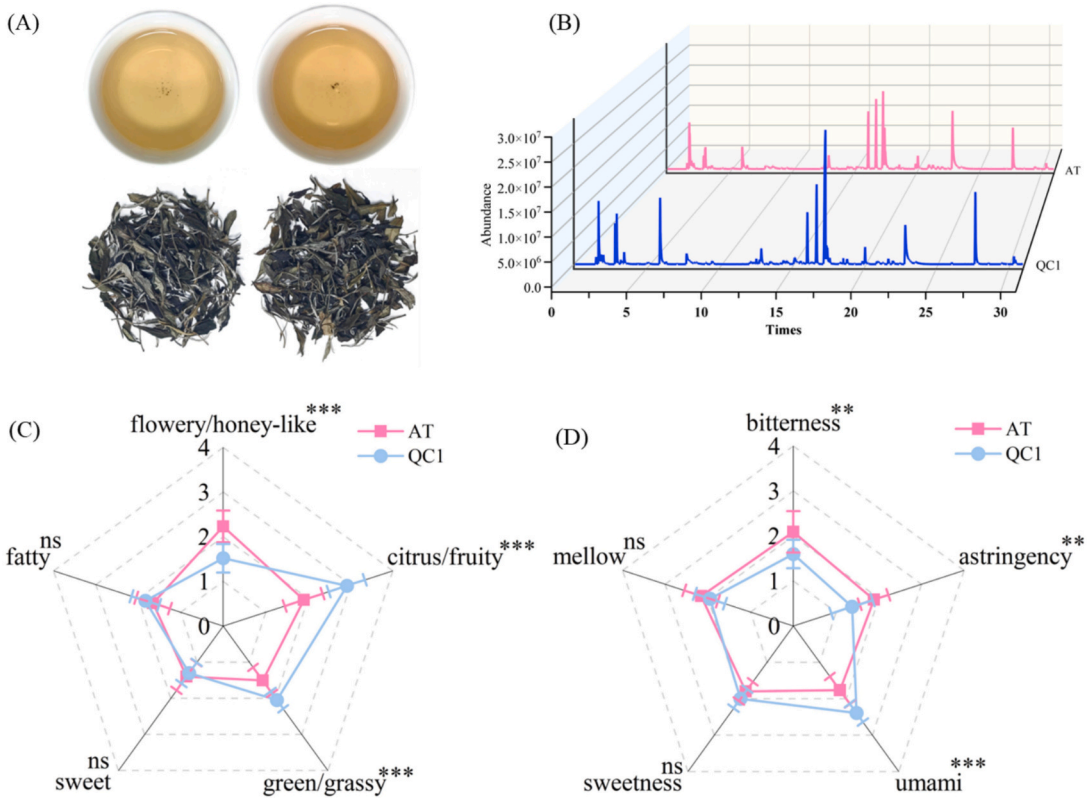

Fig. 1. (A) Dry tea leaves and their corresponding infusions of white tea (AT) and Qiancha1 white tea (QC1); (B) Total ion chromatogram of volatile compounds obtained from headspace solid-phase microextraction (HS-SPME) analysis; (C) Radar map of sensory quantitative descriptive analysis(QDA) of tea infusion aroma quality characteristics; (D) Radar map of QDA of tea infusion taste quality characteristics. ns indicates $p > 0.05$, ** indicates $p < 0.01$, *** indicates $p < 0.001$.

component analysis identified 38 compounds with significant differences ($p < 0.05$), including 24 compounds that showed highly significant variation ($p < 0.001$) (Table S2). Specifically, the AT demonstrated significantly higher levels of terpenes (45.90 vs. 43.86 μg/L), alcohols (17.67 vs. 10.09 μg/L), heterocyclic compounds (15.60 vs. 11.75 μg/L), esters (1.99 vs. 1.29 μg/L), and sulfur-containing compounds (0.93 vs. 0.53 μg/L) ($p < 0.05$). In contrast, QC1 exhibited higher levels of aldehydes (29.25 vs. 21.10 μg/L) and ketones (5.17 vs. 3.76 μg/L) ($p < 0.05$). Core aroma-active component analysis indicated that terpenes and aldehydes dominated the VOC profiles, accounting for 61.19 % and 73.54 % of the total content in the AT and QC1, respectively. These compounds were identified as the primary contributors to tea aroma. Metabolic pathway divergence was observed: terpenoid biosynthesis predominated in the AT, whereas QC1 primarily derived from fatty acid degradation-derived compounds (Zhai et al., 2022). This distinction likely reflects varietal-specific metabolic regulation.

3.3. Characterization of aroma-active compounds in AT and QC1 via GC-O-MS

This study employed the time-intensity method coupled with GC-O-MS to analyze dynamic aroma profiles. Panelists recorded aroma intensities during compound elution, with temporal intensity variations reflecting the evolving sensory characteristics of aroma compounds (Huang et al., 2022). Aroma-active compounds were identified through matching retention indices (DB-5 M capillary column), mass spectra (NIST database), and odor descriptors (Leibniz-LSB@TUM odor database). A total of 33 aroma-active compounds were detected in both samples (Table 1), primarily exhibiting floral, fruity, and fatty odors (Schuh & Schieberle, 2006). Compounds such as linalool, geraniol, decanal, neral, and citral were characterized by distinct citrus-like odor (Zhai et al., 2022). In the AT, trans-β-ionone, geraniol, citral, and β-damascenone demonstrated the highest aroma intensities (>2.8 on a 0–4 scale), whereas linalool, (Z)-4-heptenal, and trans-β-ionone dominated in AT (>2.7). These findings indicate that trans-β-ionone, geraniol, citral, β-damascenone, linalool, and (Z)-4-heptenal are key contributors to tea aroma.

Based on relative odor activity values (rOAV >1, the ratio of the relative concentration to the odor threshold) (Grosch, 2001), 10 critical aroma compounds were identified: trans-β-ionone (rOAV = 149.6), β-damascenone (47.6), (Z)-4-heptenal (44.9), geraniol (22.5), linalool (12.9), (E, Z)-2,6-nonadienal, 3-methylbutanal, 2-methylbutanal, β-myrcene, and hexanal (Table 2). Notably, trans-β-ionone exhibited an ultralow odor threshold (OT = 0.021 μg/L) and high perceived intensity (AT1 = 3.3), which dominating the floral aroma profile. β-Damascenone, with a cooked apple-like, displayed strong aroma intensity (AT = 2.8) and sensory relevance (QC1 = 2.2), serving as the core contributor to fruity odor. Despite their high perceived intensities (geraniol: AT = 3.3; linalool: QC1 = 3.2), their actual contributions were limited due to elevated odor thresholds. The synergistic effects of low thresholds and high concentrations allowed trans-β-ionone (rOAV = 149.6) and β-damascenone (rOAV = 47.6) to drive the floral and fruity odor characteristics (Grosch, 2001). Importantly, (Z)-4-heptenal (rOAV = 44.9), associated with a fish fatty-like (Yang et al., 2021), showed pronounced sensory intensity in QC1, potentially compromising aroma quality. These results highlight the pivotal role of low-threshold, high-intensity compounds (e.g., trans-β-ionone and β-damascenone) in shaping the characteristic aroma of AT.

This study integrated QDA with GC-O-MS to establish a quantitative-efficacy analytical model linking compound content, odor quality, and aroma intensity, providing a novel approach for tea aroma characterization and key compound screening. Among the 33 characteristic compounds identified, low threshold, high aroma intensity components exhibited significant leveraging effects on overall aroma perception. For

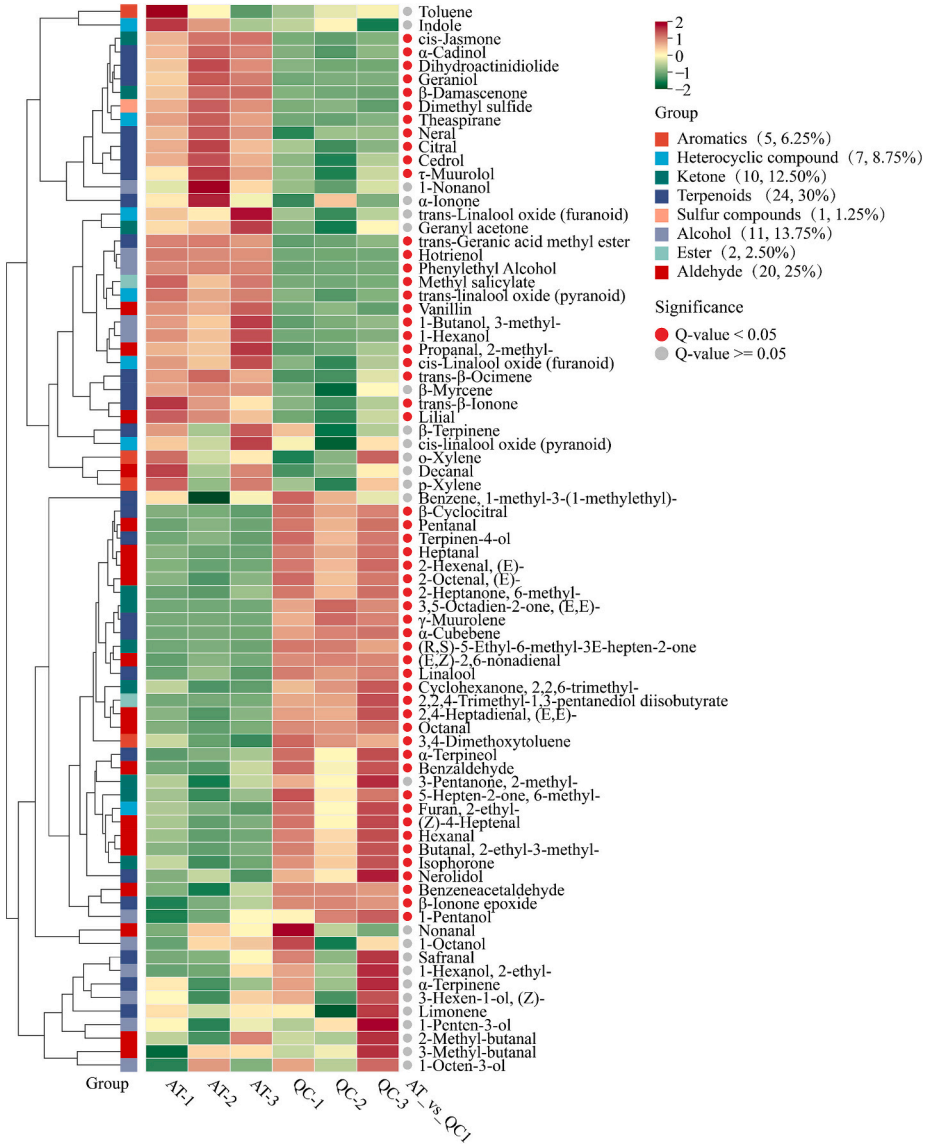

Fig. 2. Heatmap of the contents of the 79 aroma compounds in ancient tea plants white tea (AT) and '*Qiancha 1*' white tea (QC1). The numbers in the legend indicate the number of compounds and their percentage representation. Red dots to the right of the heatmap indicate significant differences ($p < 0.05$), while gray dots indicate non-significant differences ($p > 0.05$). The statistical analysis method used was the independent samples *t*-test. (For interpretation of the references to colour in this figure legend, the reader is referred to the web version of this article.)

instance, β-Damascenone demonstrated an exceptionally low sensory threshold (0.006 μg/L in water) and strong perceived intensity (2.8/2.2), which yielding a remarkably high relative odor activity value (rOAV = 13.1–4.76). This observation aligns with Grosch (2001) that trace compounds with high perceptual efficiency dominate aroma profiles (Grosch, 2001). In contrast, terpenoids such as linalool and geraniol showed comparable intensity scores (1.8–3.3) but reduced practical contributions due to their higher detection thresholds (0.6 and 1.1 μg/L in water, respectively) (Table 1 and 2), highlighting the necessity for synergistic optimization of concentration enhancement and threshold regulation in aroma quality improvement. Notably, trans-β-ionone, another terpenoid, shared similar properties with β-damascenone in terms of low thresholds (0.021 μg/L in water) and high aroma intensity (2.7–3.3), suggesting that terpenoids may exhibit dual mechanisms of synergistic enhancement or masking effects during tea flavor formation (Deng et al., 2024; Yu et al., 2021). This finding partially accounts for why terpenoids dominate both quantity and diversity among the six major tea categories (Feng et al., 2019). Consequently, dynamic equilibrium monitoring of secondary metabolites like terpenoids is crucial in tea flavor quality assessment. Recent studies have confirmed their pivotal roles in odor-odor and odor-taste interactions influencing tea flavor profiles (Deng et al., 2024; Yu et al., 2021). Future research should combine metabolomics to trace transformation pathways of key aroma precursors and employ multi-component sensory interaction models to elucidate perception mechanisms underlying complex aroma formation and cross-modal flavor interactions, thereby establishing a theoretical framework for directional modulation of tea flavor characteristics.

3.4. PCA of aroma profile differences between AT and QC1

PCA was employed to reduce the dimensionality of 79 volatile compounds. The original variables were transformed into three orthogonal principal components (PC1, PC2, PC3) with eigenvalues of 56.94, 10.31, and 5.25, respectively, meeting the Kaiser criterion (eigenvalues >1) for factor extraction (Fig. 3B). Variance decomposition (Fig. 3A) revealed cumulative contribution rates of 91.8 % (PC1: 72.1 %, PC2: 13.0 %, PC3: 6.7 %), which exceeded the empirical threshold of 85

Table 1
The odor quality and Aroma intensity perceived in the tea infusions of AT and QC1 infusions.

No	Odorants[a]	Odor quality[b]	Aroma intensity[c]		Identification[d]
			AT	QC1	
1	3-Methyl-butanal	Malty	1.8	2.0	MS, RI, O, Std
2	2-Methyl-butanal	Malty	1.8	1.8	MS, RI, O, Std
3	1-Penten-3-ol	Malty	0.7	0.8	MS, RI, O, Std
4	1-Pentanol	Malty, green	0.7	1.0	MS, RI, O, Std
5	Hexanal	Green	1.2	2.3	MS, RI, O, Std
6	(E)-2-Hexenal	Green	ns	1.0	MS, RI, O, Std
7	(Z)-3-Hexen-1-ol	Green	1.0	1.0	MS, RI, O, Std
8	(Z)-4-Heptenal	Fish oil-like	2.0	3.2	MS, RI, O, Std
9	Benzaldehyde	Bitter almond-like	ns	1.3	MS, RI, O, Std
10	1-Octen-3-ol	Mushroom-like	2.0	2.0	MS, RI, O, Std
11	β-Myrcene	Greanium-like	2.3	2.0	MS, RI, O, Std
12	Octanal	Green, soapy	0.8	0.8	MS, RI, O, Std
13	(E,E)-2,4-Heptadienal	Fatty	0.8	1.5	MS, RI, O, Std
14	Benzeneacetaldehyde	Honey	1.3	2.2	MS, RI, O, Std
15	(E)-2-Octenal	Fatty, soapy	1.0	2.0	MS, RI, O, Std
16	(E,E)-3,5-Octadien-2-one	Fatty	ns	0.8	MS, RI, O, Std
17	trans-Linalool oxide (furanoid)	Floral	2.2	1.2	MS, RI, O, Std
18	Linalool	Citrus	1.8	3.2	MS, RI, O, Std
19	Phenylethyl Alcohol	Honey	2.3	1.5	MS, RI, O, Std
20	(E,Z)-2,6-nonadienal	Cucumber-like	1.5	2.0	MS, RI, O, Std
21	cis-linalool oxide (pyranoid)	Earthy	1.0	1.2	MS, RI, O, Std
22	1-Nonanol	Soapy, fatty	1.2	1.0	MS, RI, O, Std
23	Methyl salicylate	Mint-like	1.3	0.7	MS, RI, O, Std
24	Decanal	Citrus	0.8	0.8	MS, RI, O, Std
25	Neral	Citrus	2.2	2.0	MS, RI, O, Std
26	Geraniol	Citrus	3.3	2.3	MS, RI, O, Std
27	Citral	Citrus, lemon	2.8	1.8	MS, RI, O, Std
28	β-Damascenone	Cooked apple-like	2.8	2.2	MS, RI, O, Std
29	Vanillin	Vanilla	2.2	1.3	MS, RI, O, Std
30	α-Ionone	Violet, floral	1.2	1.2	MS, RI, O, Std
31	(E)-6,10-dimethyl-5,9-Undecadien-2-one	Floral, mint	1.0	0.5	MS, RI, O, Std
32	trans-β-Ionone	Violet	3.3	2.7	MS, RI, O, Std
33	Dihydroactinidiolide	Coconut, floral	2.2	1.3	MS, RI, O, Std

a Odorants were identified in the AT and QC1 infusions. b Odor quality of each odorant at the sniffing port. c Each aroma attribute was rated on a 4-point intensity scale: weak (0–1), moderate (>1–2), and intense (>2–4). d Methods of identification: MS, odorants were identified by mass spectra; RI, retention indices; O, olfactometry; and Std, reference compounds. ns: no sniff. Ancient tea plants white tea (AT) and 'Qiancha 1' white tea (QC1).

%, indicating robust representation of original data variability (Granato et al., 2018). A two-dimensional PCA score plot (Fig. 3C) showed distinct clustering of AT and QC1 in the PC1-PC2 space, reflecting intrinsic differences in their aroma chemical fingerprints. The loading matrix (Fig. 3D) identified terpenes, aldehydes, and ketones as key discriminators for PC1 (|loading| >0.60). Negative loading values indicate inverse correlations with sample clusters, whereas positive values denote direct correlations; higher absolute values signify stronger contributions.

Sixty-one compounds dominated PC1, including β-damascenone (loading = 0.981), phenylethyl alcohol (0.97), geraniol (0.966), linalool (−0.955), dihydroactinidiolide (0.954), and trans-β-ionone (0.8). Nine compounds, such as (Z)-3-hexen-1-ol (0.976) and limonene (0.929), primarily influenced PC2. Notably, floral- and fruity-attributed compounds exhibited spatial correspondence in the PCA coordinates (Fig. 3C–D). For instance, AT clustered in the negative PC1 direction, aligning with high-loading zones for β-damascenone (cooked apple-like)

Table 2
Odor thresholds (OT) and relative odor activity value (rOAV) of key differential odourants in AT and QC1 infusions.

No	Odorants	Odor quality	OT (μg/L in water)	rOAV	
				AT	QC1
1	trans-β-Ionone	Violet	0.021[a]	149.6	124.3
2	β-Damascenone	Cooked apple-like	0.006[a]	47.6	13.1
3	(Z)-4-Heptenal	Fish oil-like	0.0087[a]	44.9	59.3
4	Geraniol	Citrus	1.1[a]	22.5	12.2
5	Linalool	Citrus	0.6[a]	12.9	22.2
6	(E,Z)-2,6-nonadienal	Cucumber-like	0.0045[a]	11.1	20.4
7	3-Methyl-butanal	Malty	0.5[a]	5.2	5.7
8	2-Methyl-butanal	Malty	1.5[a]	3.4	3.5
9	β-Myrcene	Greanium-like	1.2[a]	1.5	1.2
10	Hexanal	Green	2.4[a]	1.5	2.9
11	Benzeneacetaldehyde	Honey	5.2[a]	0.7	1.0
12	Citral	Citrus, lemon	5[a]	0.7	0.5
13	Dihydroactinidiolide	Coconut, floral	1.2[a]	0.2	0.1
14	1-Octen-3-ol	Mushroom-like	45[a]	<0.1	<0.1
15	(E,E)-2,4-Heptadienal	Fatty	150[a]	<0.1	<0.1
16	(E)-2-Octenal	Fatty, soapy	4[a]	<0.1	<0.1
17	trans-Linalool oxide (furanoid)	Floral	320[b]	<0.1	<0.1
18	Phenylethyl Alcohol	Honey	140[a]	<0.1	<0.1
19	Neral	Citrus	30[b]	<0.1	<0.1
20	Vanillin	Vanilla	53[a]	<0.1	<0.1

Odor thresholds in water from the following literature: [a] https://www.leibniz-lsb.de/en/, [b] Huang et al., 2022. rOAV, calculated as the ratio of odorant relative concentration in the AT and QC1 infusion to odor thresholds in water. Ancient tea plants white tea (AT) and 'Qiancha 1' white tea (QC1).

and geraniol (rose-like), whereas QC1 correlated with linalool (citrus-like aroma) in the same axis. These results were consistent with GC-O-MS findings (Fig. 4D), confirming that terpenoid abundance differences (e.g., β-damascenone) drive aroma divergence between the two tea samples.

3.5. Screening of differential aroma compounds between AT and QC1

An orthogonal partial least squares-discriminant analysis (OPLS-DA) model was established to identify aroma-related differential compounds. Permutation tests (n = 200) confirmed the model's validity without overfitting ($R^2Y = 0.999$, $Q^2 = 0.987$), satisfying the discrimination threshold ($Q^2 > 0.5$) (Fig. S2). Preliminary screening based on variable importance in projection (VIP ≥ 1) identified 54 potential differential compounds (Fig. 4A). A multimodal strategy integrating univariate analysis (fold change, t-test) and multivariate OPLS-DA was subsequently applied for refined selection. Fourteen significant differential compounds were identified (FDR-adjusted $p < 0.05$; Fig. 4B). Among these, seven compounds were significantly upregulated (FC = 2.05–3.68) and seven downregulated (FC = 0.08–0.49) in the AT. Compared to PCA (61 compounds) and OPLS-DA (54 compounds), this integrated approach reduced the feature set to 14 compounds, enhancing screening precision by 74.1 %. Notably, only two of the 14 compounds identified through multivariate screening—β-damascenone and methyl salicylate (aroma intensity >1, rOAV >1)—exhibited aroma activity. This outcome markedly contrasts with the QDA results, suggesting potential omissions of key odorants in the current strategy and highlighting the need for framework optimization to improve compound prioritization accuracy.

A multidimensional framework combining GC-O-MS, PCA (|PC₁ loading| > 0.6), and OPLS-DA (VIP ≥ 1.0) was further developed, ultimately identifying six key aroma compounds (Fig. 4C). RDA demonstrated that β-damascenone, geraniol, trans-β-ionone, and β-myrcene

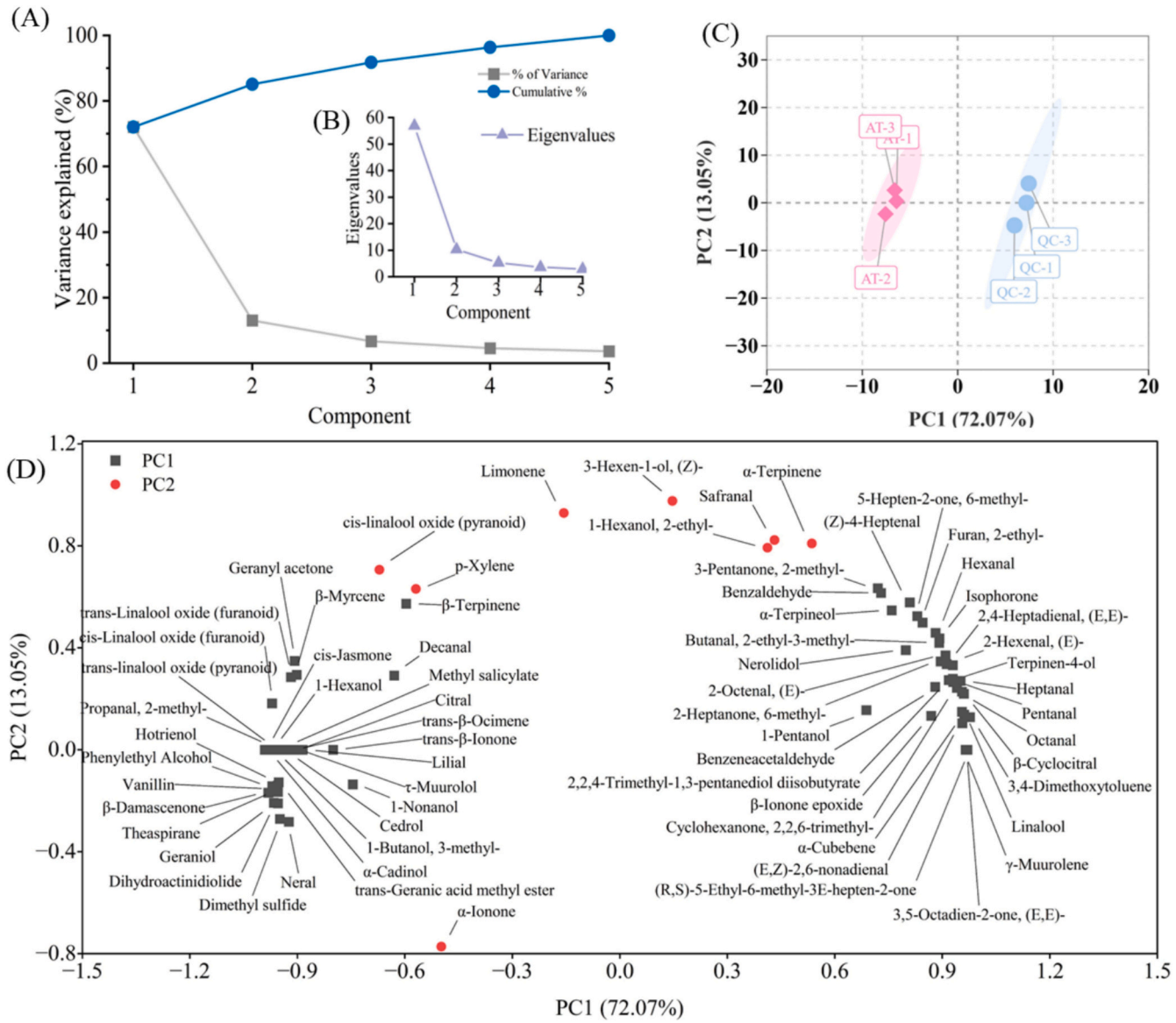

Fig. 3. (A) Explained variance and eigenvalues (B) of the first five principal components (indicating the proportion of total variance accounted for by each component); (C) Two-dimensional plots of the volatile composition of ancient tea plants white tea (AT) and '*Qiancha 1*' white tea (QC1) investigated by PCA; (D) Loading plots (Each point represents a metabolite, where larger absolute coordinate values indicate greater contributions to the principal components. Squares indicate compounds contributing to the first principal component, with absolute x-axis values >0.60; red dots represent compounds contributing significantly to the second principal component, with absolute y-axis values >0.63). (For interpretation of the references to colour in this figure legend, the reader is referred to the web version of this article.)

correlated with floral quality, whereas hexanal and (E, Z)-2,6-nonadienal were linked to fatty and green/grassy odors. These compounds collectively explained sample spatial distribution patterns (Fig. 4D). The proposed multivariate screening strategy, validated in microbial-driven aroma quality analysis of Fuzhuan brick tea, elucidates microbial metabolic mechanisms underlying flavor compound disparities and their potential for regulating biosynthesis of key flavor components (Xiao et al., 2024). This study demonstrates that integrating chemometrics (OPLS-DA, PCA) with sensory evaluations (QDA and GC-O-MS) is essential to prioritize compounds with both metabolic relevance and sensory impact, as statistical significance alone may not reflect perceptible odor contributions.

3.6. Comparative study on hypoglycemic activity and functional components of AT and QC1

α-Glucosidase, a key enzyme regulating carbohydrate digestion and absorption, delays glucose generation when inhibited (Wang et al., 2025). In vitro enzyme inhibition assays demonstrated that, at equivalent extraction concentrations (1 g/100 mL), the α-glucosidase inhibitory rate of AT extract significantly surpassed that of QC1 ($p < 0.001$; Fig. 5A), indicating that the AT extract had superior hypoglycemic potential compared to QC1. Quantitative analysis of bioactive components (Fig. 5B–C) revealed significantly higher levels in AT compared to QC1 ($p < 0.05$): esterified catechins (including EGCG, ECG, CG, and GCG) reached 222.76 mg/g (vs. 188.67 mg/g), total catechins 247.83 mg/g (vs. 215.64 mg/g), caffeine 46.65 mg/g (vs. 42.73 mg/g), and gallic acid 3.90 mg/g (vs. 3.42 mg/g). Pearson correlation analysis revealed significant positive correlations between esterified catechins and bitterness

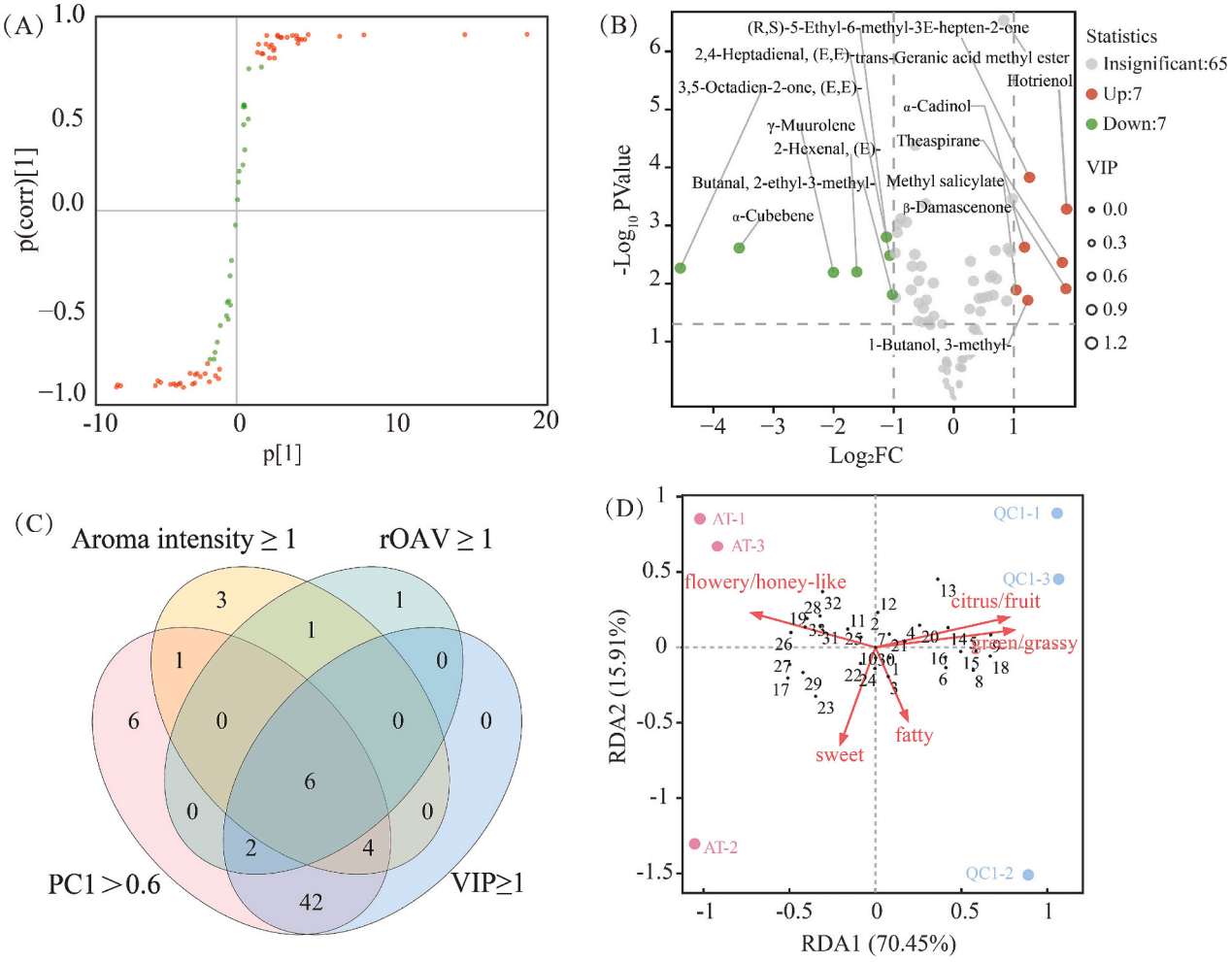

Fig. 4. (A) OPLS-DA S-plot. The x-axis represents the covariation coefficient between principal components and metabolites, while the y-axis represents the correlation coefficient between principal components and metabolites. Metabolites located closer to the upper right or lower left corners indicate more significant differences. Red dots indicate metabolites with VIP ≥ 1, while green dots represent metabolites with VIP < 1. (B) Volcano plot used for screening differential substances based on Fold-Change and Log2FC values (Fold-Change: Ratio of differences; Log2FC: Logarithm of the fold change with base 2). (C) Key odor compounds were identified by integrating the first principal component of principal component analysis (PCA), VIP > 1 in OPLS-DA, odor intensity, and relative odor activity values. (D) Redundancy analysis (RDA) was used to construct the relationships among compounds, odor quality, and samples. Numbers represent different compounds (see Table 1). Dots represent different samples, with different colors indicating different groups. Arrows indicate odor attributes, and the length of the arrows reflects the correlation between the odor and the research subject. The angle between arrows represents the strength and direction of the correlation, with acute angles indicating positive correlation and obtuse angles indicating negative correlation. (For interpretation of the references to colour in this figure legend, the reader is referred to the web version of this article.)

(r = 0.82–0.91) as well as astringency (r = 0.83–0.89) ($p < 0.05$), but negative correlations with sweetness (r = −0.82 to −0.94) and umami (r = −0.82 to −0.89) ($p < 0.05$). These components exhibited dose-dependent positive correlations with α-glucosidase inhibition (r = 0.83–0.93, $p < 0.05$). Gallic acid (r = 0.86) and caffeine (r = 0.83) also demonstrated significant positive associations with α-Glucosidase inhibitory activity ($p < 0.05$) (Fig. 5D). Molecular mechanistic studies indicate that polyphenolic compounds (e.g., EGCG) initially bind to the active site of α-glucosidase via hydrogen bonds and hydrophobic interactions. This binding subsequently induces conformational changes in the enzyme's secondary structure, leading to non-competitive inhibition of α-glucosidase activity (Dai et al., 2020; Chen et al., 2023). Caffeine may enhance polyphenol solubility via polarity modulation, thereby creating synergistic inhibitory effects (Sun et al., 2023). This multi-component cooperative mechanism not only explains the superior hypoglycemic activity of AT but also correlates with its pronounced bitter and astringent sensory profiles (Qin et al., 2024; Wang, Bo, et al., 2024; Zhang et al., 2020).

4. Conclusion

This study prepared white teas using ancient tea plants and the cultivar '*Qiancha 1*' from Yanhe County, Guizhou Province, and conducted a systematic analysis to reveal their significant differences in aroma and taste quality. QDA showed that AT exhibited significantly higher floral intensity, bitterness (2.09 vs. 1.60), and astringency (1.89 vs. 1.38) compared to QC1, demonstrated stronger citrus/grassy odor and umami. HS-SPME-GC/MS analysis detected 80 VOCs, with the total VOCs content of AT (109.50 μg/L) being significantly higher than that of QC1 (99.41 μg/L). AT showed dominance in terpenes (45.90 μg/L), alcohols (17.67 μg/L), and heterocyclic compounds (15.60 μg/L). GC-O-MS combined with QDA identified trans-β-Ionone (rOAV = 149.6, aroma intensity 3.3) and β-Damascenone (rOAV = 47.6, aroma intensity 2.8) as key aroma-active compounds in AT. These compounds, through their low thresholds and high concentrations, synergistically dominated the floral and fruity aroma characteristics. In contrast, QC1 was enriched in aldehydes (29.25 μg/L) and ketones (5.17 μg/L), with (E)-2-pentenal (0.17 μg/L, grassy) and Linalool (aroma intensity 3.2, citrus)

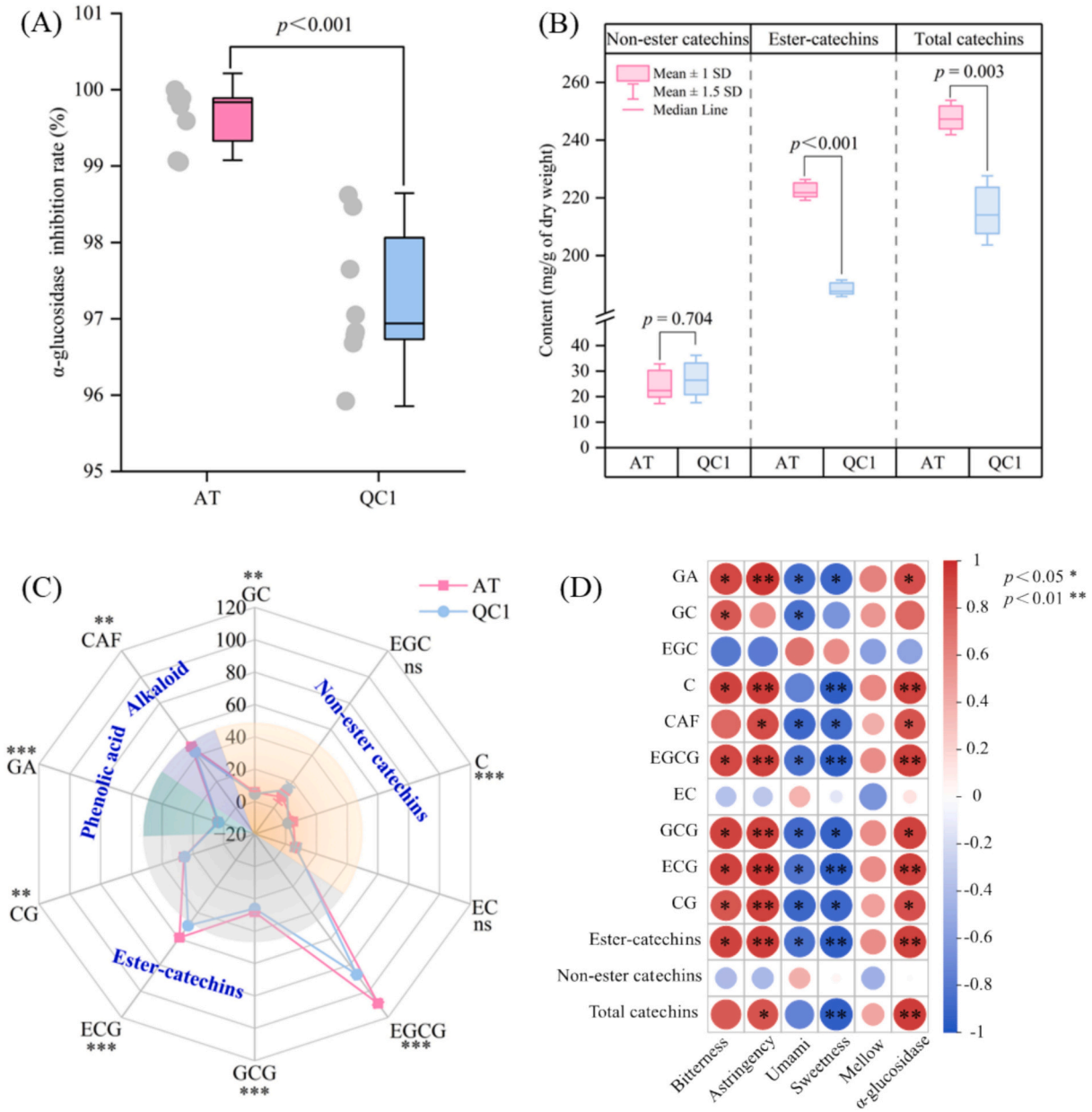

Fig. 5. (A) α-Glucosidase inhibitory activities of ancient tea plants white tea (AT) and '*Qiancha 1*' white tea (QC1) infusion samples; (B) The content of different types of catechins in AT and QC1 samples. (C) Radar map showing the contents (mg/g of dry weight) of catechins, caffeine, and gallic acid in AT and QC1 samples. (Note: The orange area represents the content of non-ester catechins, including GC, EGC, C, and EC; the gray area represents the content of ester catechins, including CG, ECG, GCG, and EGCG. (D) Correlation between non-volatile compounds content, taste characteristics, and α-glucosidase inhibitory activity. ns indicates $p > 0.05$, * indicates $p < 0.05$, ** indicates $p < 0.01$, *** indicates $p < 0.001$.

contributing to its distinct fresh and fruity odor. PCA and OPLS-DA confirmed intrinsic differences in aroma chemical fingerprints between the two teas. A subsequent multidimensional screening strategy identified six key odor-active compounds, elucidating both sample spatial distribution patterns and core mechanisms underlying aroma divergence.

In terms of taste quality, the stronger bitterness and astringency of AT correlated with its elevated levels of esterified catechins (222.76 mg/g), caffeine (46.65 mg/g), and gallic acid (3.90 mg/g) ($r = 0.82$–0.93, $p < 0.05$). Hypoglycemic activity assays revealed significantly stronger α-glucosidase inhibitory effects in AT compared to QC1 ($p < 0.001$), indicating superior antidiabetic potential. This study establishes the first flavor chemical fingerprint for AT, clarifying its quality differentiation mechanisms from the cultivated elite cultivar QC1, and provides a theoretical basis for resource authentication, metabolite-directed regulation, and functional product development. Future research should expand sample sizes across multiple harvest years and explore molecular regulatory networks of key metabolites to optimize processing techniques and enhance product quality stability.

CRediT authorship contribution statement

Shimao Fang: Writing – review & editing, Writing – original draft, Visualization, Validation, Supervision, Software, Resources, Project administration, Methodology, Investigation, Funding acquisition, Formal analysis, Data curation, Conceptualization. **Wenjing Huang:** Validation, Investigation, Formal analysis, Data curation. **Xujun Zhu:** Visualization, Validation, Investigation, Formal analysis. **Yuanchun Ma:** Formal analysis. **Jingzhou Ran:** Validation, Resources, Methodology. **Qiang Shen:** Writing – review & editing, Supervision, Resources,

Project administration. **Wanping Fang:** Writing – review & editing, Resources, Project administration, Funding acquisition.

Declaration of competing interest

The authors declare that they have no known competing financial interests or personal relationships that could have appeared to influence the work reported in this paper.

Acknowledgements

This work was supported by Guizhou Provincial Basic Research Program (Natural Science) ZK 2023 (No.165), National Natural Science Foundation of China (32460781), Science and Technology Foundation of Tongren City (202238).

Appendix A. Supplementary data

Supplementary data to this article can be found online at https://doi.org/10.1016/j.fochx.2025.102408.

Data availability

Data will be made available on request.

References

Abiri, B., Amini, S., Hejazi, M., Hosseinpanah, F., Zarghi, A., Abbaspour, F., & Valizadeh, M. (2023). Tea's anti-obesity properties, cardiometabolic health-promoting potentials, bioactive compounds, and adverse effects: A review focusing on white and green teas. *Food Science & Nutrition, 11*(10), 5818–5836. https://doi.org/10.1002/fsn3.3595

Chen, D., Dai, W. D., Gao, J. J., Hu, Z. Y., Lin, Z., Peng, J. K., & Xie, D. C. (2024). Investigations of the highly efficient processing technique, chemical constituents, and anti-inflammatory effect of N-ethyl-2-pyrrolidinone-substituted flavan-3-ol (EPSF)-enriched white tea. *Food Chemistry, 450*. https://doi.org/10.1016/j.foodchem.2024.139328

Chen, D., Gao, J. J., Peng, J. K., Wang, Z., Xu, J. Y., Zhou, M. X., & Dai, W. D. (2023). High-throughput screening and investigation of the inhibitory mechanism of α-glucosidase inhibitors in teas using an affinity selection-mass spectrometry method. *Food Chemistry, 422*. https://doi.org/10.1016/j.foodchem.2023.136179

Dai, T. T., Li, T., He, X. H., Li, X., Liu, C. M., Chen, J., & McClements, D. J. (2020). Analysis of inhibitory interaction between epigallocatechin gallate and alpha-glucosidase: A spectroscopy and molecular simulation study. *Spectrochimica Acta Part A: Molecular and Biomolecular Spectroscopy, 230*. https://doi.org/10.1016/j.saa.2019.118023

Deng, G. J., Huang, L. F., Wang, W. Y., Yu, T. Z., Ning, J. M., & Wang, Y. J. (2024). Mechanism of key volatiles in osmanthus scented green tea on the improvement of its aroma and taste quality. *Food Chemistry, 460*. https://doi.org/10.1016/j.foodchem.2024.140560

Fang, S. M., Huang, W. J., Wei, Y. M., Tao, M., Hu, X., Li, T. H., & Ning, J. M. (2019). Geographical origin traceability of Keemun black tea based on its non-volatile composition combined with chemometrics. *Journal of the Science of Food and Agriculture, 99*(15), 6937–6943. https://doi.org/10.1002/jsfa.9982

Fang, S. M., Huang, W. J., Yang, T., Pu, L. L., Ma, Y. C., Zhu, X. J., & Fang, W. P. (2024). Ancient tea plants black tea taste determinants and their changes over manufacturing processes. *LWT, 193*. https://doi.org/10.1016/j.lwt.2024.115750

Feng, Z. H., Li, Y. F., Li, M., Wang, Y. J., Zhang, L., Wan, X. C., & Yang, X. G. (2019). Tea aroma formation from six model manufacturing processes. *Food Chemistry, 285*, 347–354. https://doi.org/10.1016/j.foodchem.2019.01.174

Granato, D., Santos, J. S., Escher, G. B., Ferreira, B. L., & Maggio, R. M. (2018). Use of principal component analysis (PCA) and hierarchical cluster analysis (HCA) for multivariate association between bioactive compounds and functional properties in foods: A critical perspective. *Trends in Food Science & Technology, 72*, 83–90. https://doi.org/10.1016/j.tifs.2017.12.006

Grosch, W. (2001). Evaluation of the key odorants of foods by dilution experiments, aroma models and omission. *Chemical Senses, 26*(5), 533–545. https://doi.org/10.1093/chemse/26.5.533

Guichard, E., Barba, C., Thomas-Danguin, T., & Tromelin, A. (2019). Multivariate statistical analysis and odor–taste network to reveal odor–taste associations. *Journal of Agricultural and Food Chemistry, 68*(38), 10318–10328. https://doi.org/10.1021/acs.jafc.9b05462

Huang, H. R., Chen, X. Y., Wang, Y., Cheng, Y., Liu, Z. J., Hu, Y. C., & Xiong, Z. X. (2024). Characteristic volatile compounds of white tea with different storage times using E-nose, HS–GC–IMS, and HS–SPME–GC–MS. *Journal of Food Science, 89*(12), 9137–9153. https://doi.org/10.1111/1750-3841.17535

Huang, W. J., Fang, S. M., Wang, J., Zhuo, C., Luo, Y. H., Yu, Y. L., & Ning, J. M. (2022). Sensomics analysis of the effect of the withering method on the aroma components of Keemun black tea. *Food Chemistry, 395*. https://doi.org/10.1016/j.foodchem.2022.133549

Huang, W. J., Ye, Z. B., Wu, Y. D., Yu, T. Z., Zhao, W., Qi, Z. H., & Ning, J. M. (2025). Evaluation of taste quality of Keemun congou black tea during ripening and the effect of this quality on antioxidant capacity and in vitro inhibition of α-amylase and α-glucosidase. *Food Chemistry: X, 26*. https://doi.org/10.1016/j.fochx.2025.102264

Kong, W. L., Kong, X. R., Xia, Z. Q., Li, X. F., Wang, F., Shan, R. Y., & Chen, C. S. (2025). Genomic analysis of 1,325 *Camellia* accessions sheds light on agronomic and metabolic traits for tea plant improvement. *Nature Genetics*. https://doi.org/10.1038/s41588-025-02135-z

Lin, Y. P., Huang, Y. B., Zhou, S., Li, X. L., Tao, Y. K., Pan, Y. N., & Chu, Q. (2024). A newly-discovered tea population variety processed Bai mu Dan white tea: Flavor characteristics and chemical basis. *Food Chemistry, 446*. https://doi.org/10.1016/j.foodchem.2024.138851

Lin, Z. Y., Dai, W. D., Hu, S. S., Chen, D., Yan, H., Zeng, L., & Lin, Z. (2024). Stored white tea ameliorates DSS-induced ulcerative colitis in mice by modulating the composition of the gut microbiota and intestinal metabolites. *Food & Function, 15*(8), 4262–4275. https://doi.org/10.1039/d3fo05176e

María, J. J., Margaría, C. A., Shaw, P. E., & Goodner, K. L. (2002). Aroma active components in aqueous kiwi fruit essence and kiwi fruit puree by GC-MS and multidimensional GC/GC-O. *Journal of Agricultural and Food Chemistry, 50*(19), 5386–5390. https://doi.org/10.1021/jf020297f

Peng, J., Zhao, Y. L., Dong, M., Liu, S. Q., Hu, Z. Y., Zhong, X. F., & Xu, Z. G. (2021). Exploring the evolutionary characteristics between cultivated tea and its wild relatives using complete chloroplast genomes. *BMC Ecology and Evolution, 21*(1). https://doi.org/10.1186/s12862-021-01800-1

Qiao, D. H., Lei, W. L., Mi, X. Z., Yang, C., Liang, S. H., Li, H. K., & Wang, P. J. (2025). Three-dimensional genomic structure and aroma formation in the tea cultivar 'Qiancha 1'. *Horticulture Research*. https://doi.org/10.1093/hr/uhaf064/8042581

Qin, C. Y., Han, Z. S., Jiang, Z. D., Ke, J. P., Li, W., Zhang, L., & Li, D. X. (2024). Chemical profile and in-vitro bioactivities of three types of yellow teas processed from different tenderness of young shoots of Huoshanjinjizhong (*Camellia sinensis* var. *sinensis*). Food Chemistry: X, 24. doi:https://doi.org/10.1016/j.fochx.2024.101809.

Schuh, C., & Schieberle, P. (2006). Characterization of the key aroma compounds in the beverage prepared from Darjeeling black tea: Quantitative differences between tea leaves and infusion. *Journal of Agricultural and Food Chemistry, 54*(3), 916–924. https://doi.org/10.1021/jf052495n

Sun, Y., Cao, Q. W., Huang, Y. Y., Lu, T. T., Ma, H. L., & Chen, X. M. (2023). Mechanistic study on the inhibition of α-amylase and α-glucosidase using the extract of ultrasound-treated coffee leaves. *Journal of the Science of Food and Agriculture, 104*(1), 63–74. https://doi.org/10.1002/jsfa.12890

Tek, N. A., Ayten, Ş., Gövez, N. E., & Ağagündüz, D. (2024). Acute change in resting energy expenditure and vital signs in response to white tea consumption in females: A pilot study. *Nutrition & Metabolism, 21*(1). https://doi.org/10.1186/s12986-024-00867-z

Wang, M. T., Guo, W. W., Ke, Z. J., Mao, H. G., Lv, J. M., Qi, L. L., & Wang, J. B. (2025). Inhibitory mechanisms of galloylated forms of theaflavins on α-glucosidase. *International Journal of Biological Macromolecules, 294*. https://doi.org/10.1016/j.ijbiomac.2024.139324

Wang, T., Bo, N. G., Sha, G., Guan, Y. Q., Yang, D. H., Shan, X. Y., & Zhao, M. (2024). Identification and molecular mechanism of novel hypoglycemic peptide in ripened pu-erh tea: Molecular docking, dynamic simulation, and cell experiments. *Food Research International, 194*. https://doi.org/10.1016/j.foodres.2024.114930

Wang, Z. H., Gao, C. X., Zhao, J. M., Zhang, J. L., Zheng, Z. Q., Huang, Y., & Sun, W. J. (2024). The metabolic mechanism of flavonoid glycosides and their contribution to the flavor evolution of white tea during prolonged withering. *Food Chemistry, 439*. https://doi.org/10.1016/j.foodchem.2023.138133

Wang, Z. H., Liang, Y. L., Wu, W. W., Gao, C. X., Xiao, C. Y., Zhou, Z., & Sun, W. J. (2024). The effect of different drying temperatures on flavonoid glycosides in white tea: A targeted metabolomics, molecular docking, and simulated reaction study. *Food Research International, 190*. https://doi.org/10.1016/j.foodres.2024.114634

Wu, H. T., Sheng, C. Y., Lu, M. X., Ke, H., Li, T. H., Wei, Y. M., & Ning, J. M. (2024). Identification of the causes of aroma differences in white tea under different withering methods by targeted metabolomics. *Food Bioscience, 59*. https://doi.org/10.1016/j.fbio.2024.104020

Xiao, Y., Chen, H., Chen, Y. L., Ho, C. T., Wang, Y. L., Cai, T., & Liu, Z. H. (2024). Effect of inoculation with different Eurotium cristatum strains on the microbial communities and volatile organic compounds of Fu brick tea. *Food Research International, 197*. https://doi.org/10.1016/j.foodres.2024.115219

Yang, P., Yu, M. G., Song, H. L., Xu, Y. Q., Lin, Y. P., & Granvogl, M. (2021). Characterization of key aroma-active compounds in rough and moderate fire Rougui Wuyi rock tea (*Camellia sinensis*) by sensory-directed flavor analysis and elucidation of the influences of roasting on aroma. *Journal of Agricultural and Food Chemistry, 70*(1), 267–278. https://doi.org/10.1021/acs.jafc.1c06066

Yılmaz, H. K., Türker, M., Kutlu, E. Y., Mercantepe, T., Pınarbaş, E., Tümkaya, L., & Atak, M. (2024). Investigation of the effects of white tea on liver fibrosis: An experimental animal model. *Food Science & Nutrition, 12*(4), 2998–3006. https://doi.org/10.1002/fsn3.3980

Yu, J. Y., Liu, Y., Zhang, S. R., Luo, L. Y., & Zeng, L. (2021). Effect of brewing conditions on phytochemicals and sensory profiles of black tea infusions: A primary study on the effects of geraniol and β-ionone on taste perception of black tea infusions. *Food Chemistry, 354*. https://doi.org/10.1016/j.foodchem.2021.129504

Yu, X. M., Xiao, J. J., Chen, S., Yu, Y., Ma, J. Q., Lin, Y. Z., & Liu, R. Y. (2020). Metabolite signatures of diverse *Camellia sinensis* tea populations. *Nature Communications, 11*(1). https://doi.org/10.1038/s41467-020-19441-1

Zhai, X. T., Zhang, L., Granvogl, M., Ho, C. T., & Wan, X. C. (2022). Flavor of tea (*Camellia sinensis*): A review on odorants and analytical techniques. *Comprehensive Reviews in Food Science and Food Safety, 21*(5), 3867–3909. https://doi.org/10.1111/1541-4337.12999

Zhang, J. M., Xin, W., Zou, Y. P., Yan, J. W., Tang, W. X., Ji, Y. L., & Li, W. (2024). Dynamic changes and correlation analysis of microorganisms and flavonoids/amino acids during white tea storage. *Food Chemistry, 455*. https://doi.org/10.1016/j.foodchem.2024.139932

Zhang, L., Cao, Q. Q., Granato, D., Xu, Y. Q., & Ho, C. T. (2020). Association between chemistry and taste of tea: A review. *Trends in Food Science & Technology, 101*, 139–149. https://doi.org/10.1016/j.tifs.2020.05.015

Zhou, S., Zhang, J. M., Ma, S. C., Ou, C. S., Feng, X. Y., Pan, Y. N., & Chu, Q. (2023). Recent advances on white tea: Manufacturing, compositions, aging characteristics and bioactivities. *Trends in Food Science & Technology, 134*, 41–55. https://doi.org/10.1016/j.tifs.2023.02.016

Further reading

Lin, H. Z., Wu, L. Y., Ou, X. X., Zhou, J. J., Feng, J., Zhang, W. P., & Sun, Y. (2024). Study on the dynamic change of volatile components of white tea in the pile-up processing based on sensory evaluation and ATD-GC–MS technology. *Food Chemistry: X, 21*. https://doi.org/10.1016/j.fochx.2024.101139